Polariton amplification in a multiple-quantum-well resonant photonic crystal

S. Schumacher, N. H. Kwong, and R. Binder

College of Optical Sciences, University of Arizona, Tucson, Arizona 85721, USA
(Dated: February 1, 2008)

Based on a microscopic many-particle theory we study the amplification of polaritons in a multiple-quantum-well resonant photonic crystal. For the Bragg-spaced multiple quantum wells under investigation we predict that in a typical pump-probe setup four-wave mixing processes can lead to an unstable energy transfer from the pump into the probe and the background-free four-wave mixing directions. We find that under certain excitation conditions this phase-conjugate oscillation induced instability can lead to a large amplification of the weak probe pulse.

PACS numbers: 71.35.-y, 71.36.+c, 42.65.Sf, 42.70.Qs

INTRODUCTION – In recent years polariton amplification has been extensively studied for semiconductor quantum wells (QWs) embedded inside a planar microcavity.[1,2,3,4,5,6,7,8,9] In this Letter we address the question whether similar amplification can happen in Bragg-spaced multiple quantum wells (BSQWs) not embedded in a microcavity. In the conventional case of QWs in planar microcavities the coupling of the excitonic resonances of the QW to the optical modes confined inside the cavity leads to the formation of an in-plane (parallel to the QW plane) dispersion with lower and upper polariton branches (LPB and UPB, respectively). In the strong coupling regime this dispersion strongly differs from the bare in-plane cavity and exciton dispersions. The four-wave mixing (FWM) processes driving the amplification process in this system strongly benefit from the specific shape of the LPB that for a specific pump angle allows for triply-resonant[1,3] (phase-matched) scattering of pump-excited polaritons into pairs of polaritons in the probe and background-free FWM (BF-FWM) directions. However, also important for the polariton amplification in planar microcavities, the strong exciton-cavity mode coupling suppresses pump-induced excitation-induced dephasing (EID) from two-exciton correlations for excitation on the LPB.[10,11,12] Then, the phase-conjugate oscillation (PCO) induced gain can overcome intrinsic and EID losses to the coherently driven polarizations. This in turn brings the system above the unstable amplification threshold and enables strong amplification to occur.

Whereas in the polariton amplification in planar microcavities the propagation parallel to the plane of the embedded QW is most important, in multiple QW structures the radiative coupling of the QWs also leads to polariton effects for propagation perpendicular to the planes of the QWs.[13,14,15] However, in an arbitrarily-spaced (periodic) multiple QW structure [cf. Fig. 1(a)] the required conditions for an efficient amplification of polaritons will most likely never be met: Although a degenerate configuration – where probe and BF-FWM signals play equal roles in the amplification process [cf. Fig. 1(b)] – always allows for doubly-resonant FWM, for pump excitation close to or above the exciton resonance of the QWs additional EID from two-exciton correlations would inhibit any observation of amplification.[16]

This situation drastically changes by choosing a BSQW structure,[17,18,19,20] namely a multiple QW structure with inter-QW distances close to half the optical wavelength of the QW excitons. Then a one-dimensional resonant photonic crystal is formed with an effective polariton dispersion that is strongly modified: A sufficiently long BSQW structure exhibits an almost perfect stop-band above and below the exciton resonance of the single QWs where no propagating modes exist, cf. Fig. 1(c). However, more importantly for this work, the system exhibits effective polariton resonances at the lower and upper edges of these stop-bands where the polariton dispersion is flat.[20]
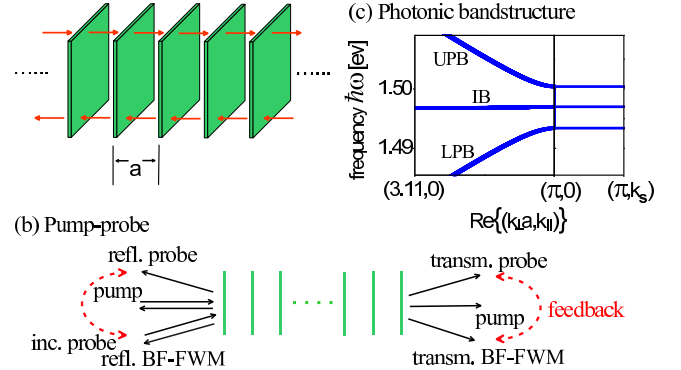
(a) Bragg-spaced multiple quantum well

FIG. 1: (color online) (a) Illustration of light propagation inside a periodic multiple quantum-well structure, including propagating and counter-propagating field components. (b) Schematic of a pump-probe geometry, including pump, probe, and background-free four-wave mixing (BF-FWM) signals. The fundamental phase-conjugate oscillation feedback between probe and BF-FWM direction leading to the polariton amplification is indicated. (c) Photonic bandstructure for an infinite Bragg-spaced multiple quantum-well structure, showing the intermediate band (IB), the stop-band regions where no light propagation inside the structure is possible, and the two polariton bands energetically above (UPB) and below (LPB) the stop-bands. The dependence of the bandstructure on the in-plane momentum $k_\parallel$ is neglected for the considered small angles of incidence related to the in-plane momentum k_s.

In this Letter we show how the polariton dispersion of a BSQW structure can lead to strong amplification of polaritons in a typical pump-probe setup. Under certain excitation conditions large time-integrated probe and BF-FWM gain and corresponding (almost) exponential signal growth over time is found in our numerical simulations.

MICROSCOPIC THEORY – Our theoretical analysis is based on a combination of a microscopic many-particle theory for the coherent optical QW response and a time-dependent transfer matrix approach to properly include the propagation of the optical fields inside the QW structure. The full numerical analysis is supported by a formal steady-state linear stability analysis focusing on those polariton-polariton interactions dominant in the amplification process. The many-particle part of our theory is formulated in the framework of the dynamics-controlled truncation approach[21,22] and includes all coherent optically-induced third order nonlinearities, i.e., phase-space-filling, excitonic mean-field (Hartree-Fock) Coulomb interaction and two-exciton correlations on a microscopic level. We use a two-band model (including spin-degenerate conduction and heavy-hole valence band) with the usual circular dipole selection rules for quasi-normal incidence for the optically induced interband transitions in the GaAs QWs.[23] Restricting ourselves to excitation spectrally below the bare exciton resonance, we account for the dominant contributions to the coherent optical response of the QWs by evaluating the polarization equations in the 1s heavy-hole exciton approximation.[24,25,26,27] The propagation of the light fields in the QW structure is included via a time-dependent transfer matrix approach that in the linear regime for an infinite BSQW structure gives the polariton bandstructure shown in Fig. 1(c).[20] To simulate a typical pump-probe setup as illustrated in Fig. 1(b) we apply an in-plane momentum decomposition of field and polarization: the pump has zero in-plane momentum $k = 0$ and we chose the finite (albeit small) in-plane momenta k_s and $-k_s$ for probe and BF-FWM, respectively. The in-plane dispersion of the excitons is neglected along with possible small changes to the polariton dispersion for probe and BF-FWM polaritons not strictly propagating in normal incidence but carrying the small in-plane momenta k_s and $-k_s$, respectively. We go beyond an evaluation of the theory on a strict $\chi^{(3)}$ level by self-consistently calculating the resulting exciton and two-exciton polarization dynamics up to arbitrary order in the optical field (the equations of motion are linearized in the weak probe field).[16,26,28] Correlations involving more than two excitons and those involving incoherent excitons are neglected. These effects are not expected to qualitatively alter the presented results for the considered coherent exciton densities of $\sim 10^{10}\,\mathrm{cm}^{-2}$ and for excitation well below the exciton resonance. Via this self-consistent solution the coupling of the probe signal to the BF-FWM signal is included which provides the basic PCO FWM feedback mechanism that can lead to instability as we
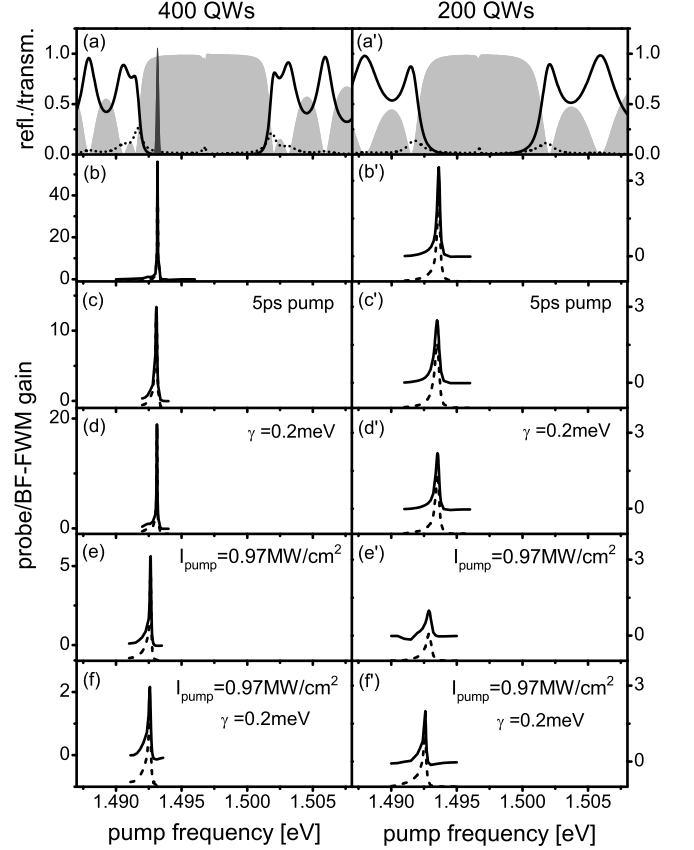

FIG. 2: Four-wave mixing induced gain in Bragg-spaced quantum wells in a typical pump-probe setup (air on both sides of the sample). Left column: 400 QWs, right column: 200 QWs. Results are shown for co-circular excitation with Gaussian pump and probe pulses of 10 ps (FWHM) and 1 ps (FWHM) length, respectively. The pump-probe delay time is zero. The pump peak intensity is $I_{\mathrm{pump}} \approx 2.49\,\mathrm{MWcm}^{-2}$, and the exciton dephasing is $\gamma = 0.1\,\mathrm{meV}$. All other material parameters are summarized in Ref. 23. Deviations from these parameters are noted in each panel. (a), (a') show the linear reflection (gray-shaded area), transmission (solid line), and absorption (dashed line) of the samples. (a) exemplarily includes the spectral shape of the pump pulse (dark-gray shaded area) for the pump frequency where the maximum gain is observed in (b). (b)-(f), (b')-(f') show the gain in the probe (solid) and background-free four-wave mixing (dashed) directions vs. the central pump frequency (same as central probe frequency). Note the different scales of the vertical axes (gain axes) in the left column.

discuss in more detail in Ref. 16. In the present study we concentrate on co-circular ($\sigma_+\sigma_+$) pump-probe excitation and keep the discussion of polarization dependencies from spin-dependent polariton scattering[29,30] for the future.

NUMERICAL RESULTS & DISCUSSION – In the framework of this theoretical approach we solve the coupled equations of motion for the optically induced probe, BF-FWM, and pump polarizations in each QW. The dynam-

ics of these polarizations is calculated self-consistently together with the time-dependent propagation of the optical fields inside the structure. Via this self-consistent solution of exciton-polarization dynamics and Maxwell's equations, the exciton-exciton interactions which are local in each QW lead to the effective polariton-polariton interaction in our theory.

From these simulations we obtain the results shown in Fig. 2 for pump-probe excitation of two BSQW structures of different lengths, containing 200 and 400 QWs, respectively. The linear optical properties are depicted in panels (a) and (a'). Panels (b)-(f) and (b')-(f') show the probe and BF-FWM gain, $(F_{\text{refl.}}^{\text{probe,BF-FWM}} + F_{\text{transm.}}^{\text{probe,BF-FWM}})/F_{\text{inc.}}^{\text{probe}} - 1$, for different pump frequencies around the lower stop-band edge and for different excitation and structural parameters as noted in each subplot and given in the figure caption. $F_{\text{refl.,transm.,inc.}}^{\text{probe,BF-FWM}}$ is the time-integrated reflected, transmitted, or incoming probe or BF-FWM intensity, respectively.

For pump excitation close to the effective polariton resonances near the lower stop-band edge, for the 400-QW structure almost two orders of magnitude of spectrally integrated probe and FWM gain are found in Fig. 2(b). This gain is strongly peaked at a specific pump frequency where excitation with the spectrally narrow pump allows for resonant pairwise scattering of pump polaritons on the polariton dispersion (blue-shifted by the repulsive polariton-polariton interaction) of probe and BF-FWM. Note that, in Fig. 2(b) this peak in the gain is spectrally narrower than the pump spectrum itself. Additional calculations, not represented in Fig. 2, show that the PCO-induced gain is sufficient to overcome intrinsic and radiative losses of the QW polarizations so that the unstable regime is reached. Once the system is unstable, the probe and BF-FWM gain grow almost exponentially with the pump length as long as the scattering into the probe and BF-FWM beams does not significantly deplete the pump. Note that strict exponential growth is only expected in a steady-state analysis, not for excitation with finite lengths pulses. Therefore in this unstable regime the gain is strongly reduced by reducing the pump length from 10 ps [panel (b)] to 5 ps [panel (c)]. Furthermore it is reduced by choosing less favorable parameters, i.e., a larger intrinsic dephasing and a lower pump intensity, as is the case in panels (c)-(f). As shown in panels (b')-(f') of Fig. 2, for the shorter 200-QW structure only moderate amounts of gain are found. Being further away from the limit of the infinite structure, the effective polariton resonances in the 200 QWs are not sufficiently pronounced to reach the unstable regime for any of the cases shown in Fig. 2.

Although the observation of large optical gain that increases with increasing pump length [cf. panels (c), (b) of Fig. 2] is indicative of the proposed instability in the BSQW structure, it does not necessarily imply exponential growth (i.e., instability) in the time domain. Therefore, we supplement the gain analysis in Fig. 2 by the time domain results shown in Fig. 3(a). These results corre-
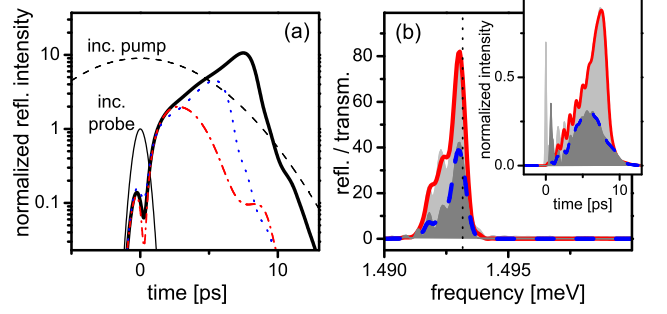

FIG. 3: (color online) (a) Time-resolved reflected probe intensity (normalized to the incoming probe's peak intensity), corresponding to the data shown in Fig. 2(b). Results are shown for pump (thin dashed line) and probe (thin solid line) central frequencies of 1.49312 eV (dashed-dotted), 1.49316 eV (solid), 1.49320 eV (dotted). (b) Spectral domain results for the probe (light-gray shaded area) and BF-FWM (solid line) reflection and probe (dark-gray shaded area) and BF-FWM (dashed line) transmission for the optimum pump frequency 1.49316 eV (indicated by the dotted line). Calculations done for a spectrally broad 200 fs probe. The inset shows the corresponding time-resolved reflected and transmitted probe and BF-FWM intensities normalized to the incoming probe's peak intensity. In the unstable regime shown, probe and BF-FWM play equal roles in the wave-mixing process dominating the system dynamics. Therefore, results for these two directions are almost indistinguishable in the plots (except for the initial probe transmission and reflection visible in the inset).

spond to the data in Fig. 2(b) around the pump frequency where the maximum gain is found. Only the probe reflection is shown since probe transmission and BF-FWM transmission and reflection show the same qualitative time dependence. Results are shown for three different pump frequencies to demonstrate the sensitivity of the time dynamics to this parameter. Close to the optimum pump frequency the time-resolved probe reflection shows (almost) exponential growth over a certain time period as long as the pump pulse is strong enough to keep the system dynamics in the unstable regime [clearly visible for the thick solid line in Fig. 3(a) between 2 and 8 ps]. Away from the optimum pump frequency the exponential growth generally has a smaller growth rate and the growth period is shorter (dotted line) or the exponential growth is absent where the unstable regime is not reached (dashed-dotted line). Note that, even in the unstable regime mono-exponential growth over time is not necessarily expected; several growing and decaying modes with different time dependencies may contribute to the total signal. In Fig. 3(b) we show spectral domain results in the unstable regime for the optimum pump frequency. Large spectral gain for probe and BF-FWM transmission and reflection is found. Its maximum is found close to the pump frequency. From this we conclude that the dominant contribution stems from (almost) degenerate FWM processes exclusively involving polaritons on the LPB.

The above-investigated instability in the BSQW is enabled by pump-excitation of the coherent polariton states at the lower stop-band edge. By the strong radiative coupling of the QWs in the structure these coherent states are spectrally well below (several meV) the exciton resonance of the single QW. This way two-exciton correlations that weaken the effective polariton-polariton scattering processes driving the instability and EID losses due to scattering off coherent excitons are strongly suppressed. Similar effects were previously pointed out for excitation of microcavity polaritons on the LPB.[10,11,12] In principle the accumulation of incoherent excitons in the QWs over time can lead to additional EID in the system which might cap the maximal achievable amount of gain with increasing pump length. However, as in the amplification of microcavity polaritons, for excitation far below the exciton resonance generation of incoherent excitons is expected to be strongly suppressed.

As noted above, the instability discussed in this paper is driven by (almost) degenerate FWM processes. In a one-dimensional non-resonant photonic crystal non-degenerate FWM involving photons on different branches of the dispersion has been used[31] to achieve efficient frequency-conversion. However, for the BSQW an instability relying on inter-branch scattering of polaritons may well be inhibited by excessive EID in the UPB.

LINEAR STABILITY ANALYSIS – Guided by the numerical results discussed above which – in the framework of our theoretical approach – include the full nonlinear polarization and field dynamics, we have also performed a linear stability analysis for monochromatic steady-state pump excitation. With the transfer matrix which relates incoming and outgoing field amplitudes in the probe and BF-FWM directions at both ends of the

multiple quantum-well structure, a temporal instability can be identified: at threshold even for zero-incoming boundary conditions non-trivial solutions for the outgoing fields exist. A similar analysis is used for example in Refs. 32,33. The following general trends could be confirmed by the linear stability analysis: Above a certain pump-induced threshold exciton density, instability is found in a small spectral window at the effective (Hartree-Fock blue-shifted) lower stop-band edge. Increasing the structure length and/or decreasing the intrinsic dephasing γ of the QW polarization generally lowers the required threshold density in agreement with the time-domain results.

CONCLUSIONS & REMARKS – Based on a microscopic many-particle theory we predict FWM instabilities in a typical pump-probe setup in Bragg-spaced multiple quantum-well structures. In contrast to the well known FWM instability in planar microcavities these instabilities are not enabled by a specific in-plane polariton dispersion but by the polariton dispersion for propagation quasi-perpendicular to the QW planes.

We note that inclusion of semiconductor to air transitions at the ends of the structure generally lowers the threshold because it effectively increases the coupling strength of the QW polarizations to the propagating fields. However, this "cavity enhancement" is not required for the reported instability. Further research, e.g., into polarization dependencies would be desirable.

[1] P. G. Savvidis *et al.*, Phys. Rev. Lett. **84**, 1547 (2000).

[2] R. Huang, F. Tassone, and Y. Yamamoto, Phys. Rev. B **61**, R7854 (2000).

[3] C. Ciuti, P. Schwendimann, B. Deveaud, and A. Quattropani, Phys. Rev. B **62**, R4825 (2000).

[4] R. M. Stevenson *et al.*, Phys. Rev. Lett. **85**, 3680 (2000).

[5] M. Saba *et al.*, Nature **414**, 731 (2001).

[6] D. M. Whittaker, Phys. Rev. B **63**, 193305 (2001).

[7] C. Ciuti, P. Schwendimann, and A. Quattropani, Semicond. Sci. Technol. **18**, 279 (2003).

[8] J. J. Baumberg and P. G. Lagoudakis, Phys. Stat. Sol. (b) **242**, 2210 (2005).

[9] J. Keeling, F. M. Marchetti, M. H. Szymanska, and P. B. Littlewood, Semicond. Sci. Technol. **22**, R1 (2007).

[10] N. H. Kwong *et al.*, Phys. Rev. B **64**, 045316 (2001).

[11] N. H. Kwong *et al.*, Phys. Rev. Lett. **87**, 027402 (2001).

[12] S. Savasta, O. Di Stefano, and R. Girlanda, Phys. Rev. Lett. **90**, 096403 (2003).

[13] L. I. Deych and A. A. Lisyansky, Phys. Rev. B **62**, 4242 (2000).

[14] T. Ikawa and K. Cho, Phys. Rev. B **66**, 085338 (2002).

[15] T. Stroucken, A. Knorr, P. Thomas, and S. W. Koch, Phys. Rev. B **53**, 2026 (1996).

[16] S. Schumacher, N. H. Kwong, R. Binder, and A. L. Smirl, submitted, arXiv.org:cond-mat/0708.0442v1 (2006).

[17] M. Hübner *et al.*, Phys. Rev. Lett. **76**, 4199 (1996).

[18] M. Scharschmidt *et al.*, Phys. Rev. B **70**, 233302 (2004).

[19] N. C. Nielsen *et al.*, Phys. Rev. B **70**, 075306 (2004).

[20] Z. S. Yang, N. H. Kwong, R. Binder, and A. L. Smirl, J. Opt. Soc. Am. B **22**, 2144 (2005).

[21] V. M. Axt and A. Stahl, Z. Phys. B **93**, 195 (1994).

[22] T. Östreich, K. Schönhammer, and L. J. Sham, Phys. Rev. Lett. **74**, 4698 (1995).

[23] Parameters used are, the background refractive index $n_{bg} = 3.61$, effective electron mass $m_e = 0.067\,m_0$, and effective hole mass $m_h = 0.1\,m_0$. The corresponding exciton binding energy is $E_b^x \approx 13\,\text{meV}$ and the bulk Bohr-radius is $a_0^x \approx 170\,\text{Å}$. For the evaluation of the theory also the 1s exciton energy $\varepsilon_x = 1.4965\,\text{eV}$, the dipole coupling $d_{cv} = 4\,e\text{Å}$, and dephasing $\gamma = 0.1\,\text{meV}$ are required. The Bragg energy used is $\varepsilon_{Bragg} = \varepsilon_x + 0.5\,\text{meV} = 1.497\,\text{eV}$.

[24] M. E. Donovan *et al.*, Phys. Rev. Lett. **87**, 237402 (2001).

[25] R. Takayama *et al.*, Eur. Phys. J. B **25**, 445 (2002).

[26] M. Buck *et al.*, Eur. Phys. J. B **42**, 175 (2004).

[27] S. Schumacher *et al.*, Phys. Rev. B **72**, 081308(R) (2005).

[28] T. Östreich and L. J. Sham, Phys. Rev. Lett. **83**, 3510 (1999).

[29] D. T. Nguyen *et al.*, Appl. Phys. Lett. **90**, 181116 (2007).

[30] S. Schumacher, N. H. Kwong, and R. Binder, submitted, arXiv.org:cond-mat/0708.1194v1 (2007).

[31] C. Becker, M. Wegener, S. Wong, and G. von Freyman, Appl. Phys. Lett. **89**, 131122 (2006).

[32] A. Yariv and D. M. Pepper, Opt. Lett. **1**, 16 (1977).

[33] W. J. Firth, A. Fitzgerald, and C. Par, J. Opt. Soc. Am. B **7**, 1087 (1990).